3 Basis of Radiopharmaceutical Localization

Shorouk Dannoon

3.1 Radiopharmaceuticals Overview

Nuclear medicine is noninvasive imaging at the cellular and molecular levels based on pathological processes. Radiopharmaceuticals (radiotracers) are given to the patient for imaging purposes. Radiopharmaceuticals are chemical compounds or biological moieties that contain radioactive element within their structures for either diagnosis or treatment. They are considered radioactive drugs. Trace amounts is administered to the patient, and the mass is extremely small. This amount is not enough to produce a pharmacologic effect and chemical toxicity is not as great of a concern as with standard pharmaceuticals.

All radionuclides used in radiopharmaceutical preparations are artificially produced. In general, the production involves a stable nuclide (target) that is bombarded with high-energy particles (neutrons or positively charged particles) to yield the radioactive nuclide of interest. The nuclear medicine radionuclides are usually obtained from a reactor, cyclotron, or generator [1]. The nuclear reactor utilizes the fast neutrons emitted from fission reaction of enriched Uranium-235 (^{235}U) [1, 2]. Enriched ^{235}U in uranium fuel rods are placed into a tank of heavy water (D_2O), which is used as a moderator for controlling fission released neutron energy. The fast neutrons are slowed down to thermal energy by their interaction with D_2O. The thermal neutrons are easily captured by other Uranium atoms to initiate additional fission reactions and this chain reaction maintains the flux of neutrons. The rate of nuclear fission is controlled by the position of control rods. The control rods are made of Cadmium or Boron that have a high cross-section for absorbing neutrons. The production of neutron activated radionuclide is achieved by introducing the target material (stable nuclides) through ports into the neutron flux in the D_2O tank. To insure the safety of the surroundings, the whole reactor is shielded with concrete [1, 2].

As for cyclotrons, they are a type of particle accelerator invented by Ernest O. Lawrence in 1932 in which charged particles accelerate outward from the center along a spiral path. The particles (protons) are held in a spiral path by a static magnetic field and accelerated by a rapidly varying electric field. Stable, nonradioactive isotopes are placed inside the cyclotron, then the accelerated charged particles (protons) bombard the stable isotopes creating radioactive isotopes for nuclear medicine and other purposes [1, 3].

On the other hand, generators are more convenient method of obtaining medical radionuclides with short half-lives [1, 4]. They consist of a longer lived parent radionuclide that is loaded onto a column that decays to the daughter radionuclide.

S. Dannoon (✉)
Department of Nuclear Medicine, Faculty of Medicine, Kuwait University, Kuwait City, Kuwait
e-mail: shorouk.dannoon@ku.edu.kw

A. H. Elgazzar (ed.), *The Pathophysiologic Basis of Nuclear Medicine*,
https://doi.org/10.1007/978-3-030-96252-4_3

The parent and daughter radionuclides are chemically different that the daughter is removed from the column by elution with a solvent while the parent stays absorbed to the column. Upon elution of the daughter radionuclide, the parent radionuclide decays to build up more daughter radionuclide until the parent activity is depleted [1, 4]. The column is shielded in lead. To date are useful medical radionuclide generators which are: ^{99}Mo/^{99m}Tc, ^{68}Ge/^{68}Ga, ^{82}Sr/^{82}Rb,^{90}Sr/^{90}Y and ^{188}W/^{188}Re.

Radionuclide can be introduced into a drug in different approaches. Isotopic labeling involves the substitution of a stable nuclide with its radioactive isotope creating a radioactive analogue [5]. The radioactive analogue has similar chemical and biological properties to the stable parent compound. Therefore, the radioactive analogue will be a physiological tracer. However, the nonisotopic labeling approach involves incorporating a radioactive nuclide that was not previously present in the parent compound [5]. The majority of the radiopharmaceutical in clinical practice today are the nonisotopic labeled compounds. The nonisotopic labeled radiopharmaceuticals split into two different categories: essential and tagged radionuclide. The essential is also referred to as integrated radionuclide. In this labeling method, the radionuclide is an important component in the overall structure of the drug, without it the drug will not have the same biodistribution. The chelation of the radionuclide to the ligand results in the desired complex. The majority of the earlier radiopharmaceuticals were the integrated ones. More recently, the work has been toward production of target-specific radiopharmaceuticals to minimize the unnecessary radiation exposure to the body during imaging or radiotherapy. The most convenient approach is to incorporate radiometals to receptor-specific molecules such peptides, antibodies, and antigens. The radionuclide is attached to the biological molecule via a bifunctional chelate (BFC), which can hold the radiometal tightly and at the same time form a stable conjugation with the active groups of the biological molecule. In this method, the radionuclide is being tagged along till the biological molecule reaches its target.

Radiopharmaceuticals have been used in diagnostic and radiotherapeutic agents. There are two types of diagnostic radiopharmaceutical. Single photon emission computed tomography (SPECT) radiopharmaceuticals that contain gamma emitting radioisotopes. Positron emission tomography (PET) radiopharmaceuticals that contain positron emitting radioisotope. While therapeutic radiopharmaceuticals contain auger electrons, β^- or α particles that are known to be highly ionizing as they are non-penetrating radiation, so they deliver cytotoxic doses to diseased sites, resulting in the death of the cells.

3.2 Mechanisms of Radiopharmaceuticals Localization

The uptake and retention of radiopharmaceuticals by different tissues and organs involve many different mechanisms, as summarized in Table 3.1. The pharmacokinetics, biodistribution, and metabolism of the radiopharmaceutical are very important to understanding the mechanisms of radiopharmaceutical localization in the organ or tissue of interest. Injury to a cell or tissue significantly alters the morphology and molecular biology compared with that of normal tissue or organs.

3.2.1 Compartmentalized Localization

Compartmentalized localization is when molecules of interest are spread in an enclosed volume or space.

- Uniform distribution within a compartment.

  The model example of uniform dispersion within a compartment is the blood pool. The quantitative determination of blood volume can be done using the tracer dilution method. Radioiodinated human serum albumin with I-125 (I-125 HSA) is used to determine plasma volume because it is a radiopharmaceutical that diffuses in the

Table 3.1 Mechanisms of radiopharmaceuticals' localization

Localization mechanism	Radiopharmaceuticals
Compartmentalized localization	^{125}I-HAS, ^{125}Cr-RBC, ^{99m}Tc-RBC, Xe-133, ^{111}In-DTPA, ^{99m}Tc-DTPA, ^{99m}Tc-Sulfur-colloid
Passive diffusion	^{99m}Tc-DTPA (brain), ^{99m}Tc-HMPAO, ^{99m}Tc-ECD, ^{99m}Tc-sestamibi, ^{99m}Tc-tetrofosmin, [^{13}N]NH_3,^{67}Ga-citrate, [^{18}F]FDOPA, [^{18}F]FMISO
Facilitated diffusion	[^{18}F]FDG, ^{99m} Tc-disofenin and mebrofenin, ^{99m}Tc (V) DMSA (MTC)
Active transport	$^{123}I^-$ and $^{131}I^-$, $^{99m}TcO_4^-$(Thyroid), $^{201}Tl^+$, $^{82}Rb^+$, ^{123}I-MIBG, ^{99m}Tc (III) DMSA (Renal), [^{18}F]FACBC, [^{18}F]FLT, [^{18}F]FET, [^{18}F]Choline and [^{11}C]Choline
Filtration	^{99m}Tc-DTPA (renal), ^{99m}Tc-MAG_3, ^{125}I-iothalamate, and ^{51}Cr-EDTA
Secretion	$^{99m}TcO_4^-$(stomach), ^{99m}Tc-MAG_3
Phagocytosis	^{99m}Tc-sulfur colloid
Cell sequestration	Denatured ^{99m}Tc-RBC
Capillary blockade	^{99m}Tc-MAA
Ion exchange	$^{89}Sr^{2+}$, $^{18}F^-$
Chemisorption	^{99m}Tc-MDP, ^{99m}Tc-HDP, ^{153}Sm-EDTMP
Cellular migration	^{111}In-oxine-WBC, ^{99m}Tc-HMPAO-WBC
Receptor binding	^{68}Ga-DOTA-PSMA, ^{18}F-PSMA, ^{131}I-tositumomab and ^{111}In/^{90}Y-ibritumomab tiuxetan, ^{111}In-octreoscan, ^{68}Ga-DOTA-octreotide, ^{64}Cu-DOTA-tyr^3-octreotate, [^{18}F] Florbetapir, [^{18}F]Florbetapir, [^{18}F]flutemetamol, [^{18}F]FES, [^{123}I]ioflupane (DaTscan)

plasma [6, 7]. Red blood cells (RBC) radiolabeled with Cr-51 is a radiopharmaceutical that diffuses within the cellular content of blood, so it is used to determine red cell volume/mass [7, 8]. Tc-99m labeled RBCs are dispersed in the blood and used in gated blood pool imaging of left ventricular wall motion and determination of left ventricular ejection fraction [9].

- Nonuniformities within a compartment.

  In certain incidents, radiopharmaceuticals may have nonuniform distribution within the compartment due to pathological condition. For example, a localized area of increased ^{99m}Tc-RBCs activity can be caused by increased blood volume in a hemangioma [10, 11].

  In other situations, areas of decreased radiopharmaceutical concentration are usually the result of an obstruction in a compartmental space. In a complete obstruction in the lung airways demonstrated by Xe-133 ventilation, then there will be absence of Xe-133 in the area beyond the site of airway obstruction [12, 13]. If partial obstruction (common in COPD), then there will be absence of Xe-133 in the affected area upon initial inhalation and breath-hold, but Xe-133 gas will pass through the site(s) of partial obstruction over time during equilibrium rebreathing [14].

  As for In-111-pentetate (DTPA), it can diffuse freely in the extracellular fluid and can accumulate in lesions with defects in Blood Brain Barrier (BBB). Obstructions can also occur in the CSF space. Both ^{99m}Tc-DTPA andIn-111-DTPAcan be used for the assessment of BBB disruption as it localizes in areas within the cranium that had been disrupted by infection, neoplasms, trauma, or stroke [15, 16]. ^{99m}Tc-DTPA is a nondiffusible tracer for evaluation of BBB permeability, similar to ^{99m}Tc-pertechnetate and ^{99m}Tc glucoheptonate. ^{99m}Tc-DTPA brain scintigraphy has been used in the past to detect brain infarcts as well as brain metastases [15, 16].

  An obstruction in the cystic duct of the biliary tract will be visualized due to decrease of radiopharmaceutical in the gallbladder, and if the common bile duct is obstructed, there will be decrease of radiopharmaceutical in the small intestine. Tc-99m hepatobiliary radiopharmaceuticals, disofenin (DISIDA), and mebrofenin (BRIDA), are excreted from the liver into the bile and flow through the biliary tract with normal flow into the gallbladder and into the intestine [17].

- Leakage from the compartment.

  In some pathological conditions there could be an abnormal leakage from the compartment, and radiopharmaceuticals can detect and identify the location of this leakage. For example, gastrointestinal hemorrhage (GI bleeding), blood leaks from the vasculature and accumulates in the GI tract and Tc-99m RBCs can be used to detect the site of the GI bleeding [18, 19].
- Movement/flow within a compartment.

  In some pathological conditions, there may be a change in the direction, rate and extent of flow within a compartment. Tc-99m sulfur colloid is the preferred radiopharmaceutical for determining the rate of emptying of gastric contents into the intestine because it is not absorbed by the GI tract. Tc-99m sulfur colloid bound in scrambled eggs can be used to evaluate gastric empting of food solids while Tc-99m sulfur colloid mixed in water or other liquid such as juice that can be used to evaluate gastric emptying of liquids [20, 21]. Individual patient gastric emptying is compared to normal values.

3.2.2 Passive Diffusion

Passive diffusion is the movement of molecules from high to low concentration to achieve even concentration (chemical equilibrium). In biological systems, passive diffusion usually involves the ability of molecules to cross the phospholipid membrane so these molecules should be highly lipid soluble and be in a neutral state not charged under physiological pH conditions. Also, their molecular size should be small enough to pass through the small pores of the membrane. The molecule movement across the membrane is simply a molecular motion and does not require additional energy, transporters, carriers, or receptors. The passive diffusion is nonselective, noncompetitive, and not subjected to saturation.

A classic example of passive diffusion in nuclear medicine is ^{99m}Tc-DTPA brain imaging. ^{99m}Tc-DTPA cannot normally penetrate the blood–brain barrier (BBB) that is made of endothelial cells of the cerebral vessels form a continuous layer without gap junctions preventing the diffusion of hydrophilic (water-soluble) molecules. So normally, ^{99m}Tc-DTPA remains in the blood pool until cleared by the kidneys. In conditions that result in disruption of the BBB, such as tumor, stroke, and infection, the ^{99m}Tc-DTPA can diffuse across the disrupted BBB and accumulate in that affected area of the brain [15, 16].

Intact BBB allows the transport of small molecules across the plasma membrane of the neuron by facilitated diffusion. However, diffusion is not a unidirectional process, and there is a need for accumulation and retention of radiopharmaceuticals at the site of interest in order to take a meaningful image. The localization of the cerebral perfusion radiopharmaceuticals ^{99m}Tc-exametazime (HMPAO) and ^{99m}Tc-bicisate (ECD) which are lipophilic radiotracers, involve the delivery via cerebral arterial blood flow, diffusion into the brain and retention in the brain due to conversion to a more stable hydrophilic molecule and enzymatic metabolism, respectively [22, 23] (Fig. 3.1).

^{99m}Tc-myocardial perfusion agents involve the delivery by blood flow through the coronary arteries, diffusion into myocardial cells and retention in those cells [24, 25]. Both ^{99m}Tc-sestamibi and ^{99m}Tc-tetrofosmin cross the cell membranes by lipophilic diffusion and then are retained by electrostatic binding to negative electrical charges on the mitochondrial membranes in normal cells when Ca^{2+} are significantly low [26]. In cases of irreversible ischemia when extracellular levels of Ca^{2+} enters the cell and binds to the mitochondria, Tc-myocardial perfusion agents are blocked from binding to the mitochondria.

$[^{13}N]NH_3$, as a nonionic form, is freely permeable to all cell membranes. It diffuses across the myocardial cell capillary membrane, then is converted to N-13 glutamine by glutamine synthetase, and subsequently is trapped within tissues by incorporation in the cellular pool of amino acids [27, 28]. Myocardial uptake is proportional to coronary blood flow. The linear relationship between distribution of $[^{13}N]NH_3$ and the regional blood perfusion allows for the imaging and measurement of cerebral and myocardial blood flows [27, 28].

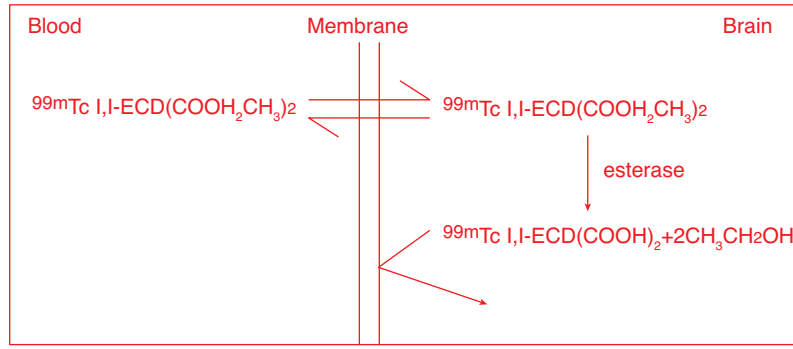

Fig. 3.1 ^{99m}Tc-ECD is a neutral, lipophilic complex that can cross the BBB via passive diffusion. It is retained in the brain after undergoing enzymatic hydrolysis of one of the ester functions to become an ionized metabolite by esterase enzyme

^{67}Ga-citrate is known to localize in tumors and inflammatory lesions. It is speculated based on in vivo studies, that free and unbound ^{67}Ga-citrate diffuse into the cells and once within the cells, ^{67}Ga binds to iron-binding proteins such as lactoferrin and ferritin preventing back-diffusion of free ^{67}Ga [29, 30].

[^{18}F]Fluorodopa ([^{18}F]FDOPA) is neutral and capable of crossing the BBB. Up on crossing the BBB, [^{18}F]FDOPA is decarboxylated by cellular aromatic amino acid decarboxylase (AAAD) to form fluorodopamine (FDA) which remains within the neuron. [^{18}F]FDOPA selectively localize within the basal ganglia of the brain in the area that controls movement. [^{18}F]FDOPA targets the presynaptic dopaminergic function in the brain. In degenerative diseases such as Parkinson's disease, there is loss of dopaminergic neurons, so there will be less accumulation of [^{18}F]FDOPA in the basal ganglia than a healthy, age-matched control. [^{18}F]FDOPA has other applications, it can accumulate in vivo within tumors and in evaluation of pheochromocytoma and thyroid carcinoma due to the increase utilization of amino acid by the cancerous lesions [31–33].

^{18}F-Fluoromisonidazole ([^{18}F]FMISO) diffuses freely into all cells. However, it accumulates in viable hypoxic cells, diffuses out of normoxic cells and is not retained in necrotic cells. Upon entering a viable cell, ^{18}F-MISO is in an environment where electron transport is taking place, the NO_2 substituent (which has a high electron affinity) takes on an electron to form the radical anion reduction product. If O_2 is also present, that electron is rapidly transferred to oxygen and ^{18}F-MISO changes back to its original structure and can leave the cell [34, 35]. However, in the absence of O_2 in hypoxic cell, a second electron reacts with the nitroimidazole (radical anion reduction product) to form a 2-electron reduction product then the reduced [^{18}F]FMISO reacts nondiscriminately with peptides and RNA within the cell and gets trapped. Therefore, the retention of [^{18}F]FMISO is inversely related to the intracellular partial pressure of O_2 [34, 35].

3.2.3 Facilitated Diffusion

Facilitated diffusion requires a carrier to transport a molecule across the membrane. Carriers are selective and only specific molecules fit into them. Therefore, there is competition with similar molecules that fit into this carrier and due to limited number of carriers, it is possible to reach saturation. However, facilitated diffusion utilizes carriers that are passive, so it does not require external energy but needs a concentration gradient to operate. This mechanism allows the transport of molecules in either direction through the membrane based on the concentration of gradient. The most commonly used PET radiotracer, F-18 flurodeoxyglucose ([^{18}F]FDG), is transferred into the cell through facilitated diffusion mechanism. [^{18}F]FDG, is a radiolabeled analogue of D-glucose (Fig. 3.2), so it enters the cell via transmembrane protein transporters [GLUT] similar to glucose. Cellular uptake of [^{18}F]FDG reflects the glucose metabolism so glucose and [^{18}F]FDG are competing for the same GLUT transporters, and elevated

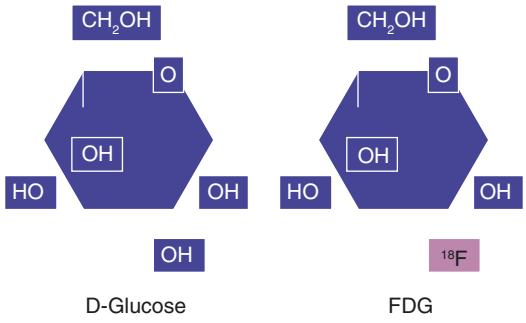

Fig. 3.2 [^{18}F]FDG is an analogue of D-glucose. The hydroxyl group at the second position in D-glucose is replaced by F-18 in [^{18}F]FDG

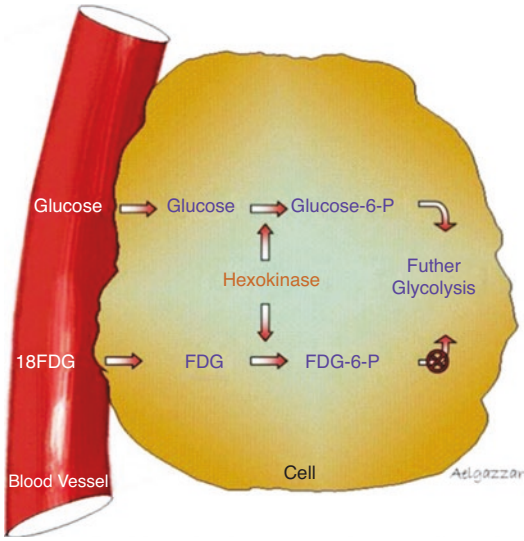

Fig. 3.3 Both of glucose and [^{18}F]FDG are transported into the cell via Glut transporters. Upon entering the cell, both undergo phosphorylation at the 6 position by hexokinase. Phosphorylated-glucose will undergo additional enzymatic steps, however, phosphorylated-[^{18}F]FDG at the 6 position does not and becomes trapped inside the cell.

blood levels of glucose will decrease cellular uptake of [^{18}F]FDG. Once inside the cell, both glucose and [^{18}F]FDG are phosphorylated by hexokinase resulting in Glucose-6-phosphate and [^{18}F]FDG-6-phosphate, respectively (Fig. 3.3). Glucose-6-phosphate enters the glycolytic pathway but [^{18}F]FDG-6-phosphate is blocked and is retained in the cell as it does not fit in the GLUT to diffuse out, and this is referred to as metabolic trapping. [^{18}F]FDG-6-phosphate may be converted back to [^{18}F]FDG, however the enzyme responsible for such a conversion is present in very low concentration or not present all in cancer tissue allowing for better images of oncological patients. [^{18}F]FDG accumulated in granulomatous tissue and macrophages so it has been used to image infection and inflammation as well [36–39].

On the other hand, the hepatocytes in the liver extract substances from the blood and secrete them into the bile. ^{99m}Tc labeled tracers like disofenin and mebrofenin diffuse through pores in the endothelial lining of the sinusoids, bind to the anionic membrane-bound carriers on the hepatocyte and secreted into the bile similar to bilirubin [40].

At alkaline pH (pH 8–9), ^{99m}Tc forms a pentavalent complex with DMSA (^{99m}Tc (V) DMSA). This complex mimics phosphate ion and is rapidly excreted in the urine. It localizes in a number of tumors such as medullary thyroid carcinoma (MTC), bone metastases and other bone lesions. Its uptake is dependent on extracellular Na^+ concentration, indicating the importance of sodium-dependent transporter in ^{99m}Tc (V) DMSA uptake [15].

3.2.4 Active Transport

Active transport utilizes carriers to transport molecules across membranes but unlike facilitated diffusion it requires energy such as ATP. By using energy to transport molecules across the membrane, molecules can be transported against a concentration gradient. Since a carrier is used, it is selective and only specific molecules that fit the carrier will be transported across the membrane. Therefore, there is competition with similar molecules that fit into this carrier and due to limited number of carriers, it is possible to reach saturation.

One of the first active transport radiotracers in Nuclear Medicine is the concentration of iodide in the thyroid gland. Radioisotopes of iodine such as $^{123}I^-$ and $^{131}I^-$ are useful radiopharmaceuticals to evaluate thyroid function. Iodide ions are transported into thyroid cells via the Na^+/I^- symporter. In the thyroid, iodide is oxidized to iodine and

becomes bound to tyrosine which is transformed to the thyroid hormones [41–44]. In addition, Tc-99m-pertechnetate ($^{99m}TcO_4^-$) accumulates in the thyroid similar to iodide since it has a negative charge and similar ionic size [44]. Presence of iodide in the blood from iodine containing medications or iodine contrast agents will compete with these radiopharmaceuticals for thyroid uptake resulting in poor image quality.

Another well-known example of active transport is the Na^+/K^+ pump, especially of importance in the heart muscle. Thallous chloride ($^{201}Tl^+$) has been used for myocardial perfusion scans. $^{201}Tl^+$ is a radiometal so it is not an analogue of K^+ but it has a similar ionic radius, a single positive charge and fits in the Na^+/K^+ pump [45–47]. Uptake in heart muscle demonstrates viability. The delivery to the myocardial cells is by blood flow through the coronary arteries so the heart muscle uptake reflects coronary perfusion. It has been also used for tumors such as brain tumors, osteosarcomas low-grade lymphomas, Kaposi sarcomas, and parathyroid tumors [45, 46]. This accumulation is a function of blood flow and active transport system of Na^+/K^+ pump within cell membrane. The uptake can be inhibited by blocking the Na^+/K^+ pump with ouabain, digitalis and furosemide [48, 49]. A PET myocardial perfusion radiotracer is rubidium chloride ($^{82}Rb^+$). $^{82}Rb^+$ is a chemical analog of potassium as it falls immediately below it on the periodic table. $^{82}Rb^+$ fits in the Na^+/K^+ pump and its uptake is similar to $^{201}Tl^+$ [48].

I-123-metaiodobenzylguanidine (^{123}I-MIBG) is an analog of noradrenaline. It fits in the prenorepinephrine transporter (adrenergic presynaptic neurons) in adrenergic nerve terminals. Norepinephrine transporter is a transmembrane carrier that transports monoamine neurotransmitters into neurons where they are accumulated in storage vesicles. These transporters are over expressed on certain neoplasms such as neuroblastoma, pheochromocytoma, medullary thyroid carcinoma, retinoblastoma, melanoma and bronchial carcinoma [49, 50].

At acidic pH (pH 2–3), ^{99m}Tc forms a trivalent complex with DMSA (^{99m}Tc (III) DMSA). ^{99m}Tc-DMSA accumulates in proximal tubular cells of kidneys and thereby used for renal cortical imaging. ^{99m}Tc-DMSA is filtered as bound to α1-microglobulin and accumulates in the kidneys by megalin/cubilin-mediated endocytosis of the ^{99m}Tc-DMSA protein complex. Renal accumulation of ^{99m}Tc-DMSA is dependent on megalin/cubilin receptor function and therefore is a marker of proximal tubule endocytic activity [51–53].

Fluciclovine, anti-1-amino-3-^{18}F-fluorocyclobutane-1-carboxylic acid ([^{18}F]FACBC). [^{18}F]FACBC is for men with suspected prostate cancer recurrence based on their elevated prostate specific antigen (PSA) levels. [^{18}F]FACBC takes advantage of the increased amino acid transport in prostate cancer cells, and it is taken up by the L-amino acid transporter and alanine-serine-cysteine transporter systems. These transporters are unregulated in prostate cancer and are associated with more aggressive disease. Once inside the cell, [^{18}F]FACBC does not undergo metabolism and the amino acid transporters mediate influx and efflux of amino acids, so [^{18}F]FACBC washout occurs over time [54–57]. Therefore, early imaging is recommended to maximize lesion uptake.

^{18}F-Fluorothymidine ([^{18}F]FLT) is utilized to measure cellular proliferation as the concentration of [^{18}F]FLT in cells is proportional to cellular proliferation. It is transported from the blood into cells by active transport. Once in the cell, [^{18}F]FLT is a substrate for thymidine kinase I (TK1) and is phosphorylated but not incorporated into DNA (Fig. 3.4). Phosphorylated FLT cannot exit

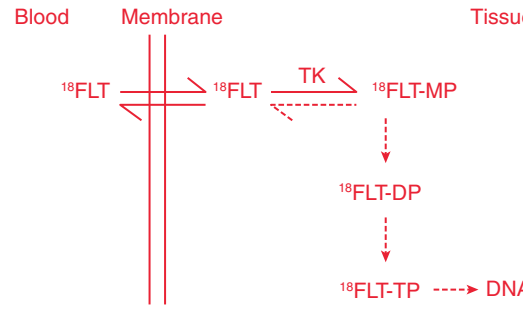

Fig. 3.4 Upon entering the cell via an active transport mechanism, [^{18}F]FLT undergoes phosphorylation by TK1. Phosphorylated-[^{18}F]FLT does not exit the cells and its concentration in cells is proportional to cellular proliferation

the cell. One advantage of [^{18}F]FLT is that it is only a substrate for TK1 and not for mitochondrial TK2 and so it is a more specific tracer compared with other fluorinated tracers for cellular proliferation [58, 59].

^{18}F-Fluoro-Ethyl-Tyrosine ([^{18}F]FET), is an amino acid analog and it reflects the increased amino acid transport of tumor cells. It is a neuro-oncologic PET radiotracer. It is actively taken up in tumor cells via amino acid transport system L. It is neither incorporated into proteins nor readily degraded, resulting in high intracellular concentrations [60]. Radiolabelled amino acid-based agents are useful in PET brain tumor imaging because [^{18}F]FDG is somewhat insensitive for detecting tumors and lesions in the brain due the high levels of glycolytic metabolism in the normal cortex and white matter [61].

[^{18}F]Choline and [^{11}C]Choline target the cellular membrane phospholipids. They enter the cell through choline transporters with accumulation in tumors due to malignancy-induced overexpression of choline kinase (CK) that catalyzes the phosphorylation of choline to form phosphorylcholine followed by generation of phosphatidylcholine in the tumor cell membrane [62–65]. They have been approved for recurrent prostate cancer detection.

3.2.5 Filtration

Filtration is a passing of molecules through pores or channels due to hydrostatic or osmotic pressure gradient. The molecular size vs. pore size and availability are the most important factors in filtration. In addition, filtration requires a force or pressure gradient, it does not require external energy or carriers. Filtration is not competitive so it is not subjected to saturation. Glomerular filtration by the kidney is the prime example of filtration to estimate the function of the renal tissue. Only small hydrophilic molecules (i.e., molecular weight of <5000) can pass through the glomerular pores, and only the ones that are free in plasma (not bound to proteins) are available to be filtered, and these molecules should not be able to be secreted or reabsorbed by tubule. Blood pressure is the pressure gradient for glomerular filtration. Even though many radiopharmaceuticals are excreted by glomerular filtration, ^{99m}Tc-DTPA, ^{99m}Tc-MAG$_3$, ^{125}I-iothalamate, and ^{51}Cr-EDTA are the radiopharmaceuticals that are mainly used for glomerular function renal imaging studies [66–69].

3.2.6 Secretion

Secretion is active transport of substances out of glands and other tissues. For example, the secretion of hydrochloric acid (HCl) by the stomach, secretion of H^+, K^+, NH_3, urea, creatinine or histamine by the kidney tubular cells into the urine, and secretion of bilirubin by the liver into the bile. In Meckel's Diverticulum, a patch of ectopic stomach tissue is usually found in the intestine, so it may secrete hydrochloric acid (HCl) that erodes the intestinal wall, which leads to bleeding. Tc-99m-pertechnetate (TcO_4^-) is negatively charged and of similar size as chloride (Cl^-), so it is secreted as pertechnic acid ($H^+TcO_4^-$) by both normal stomach tissue and Meckel's Diverticula [70, 71].

As for the kidneys, the tubular cells secrete some waste products into the urinary collecting system. ^{99m}Tc-mertiatide (^{99m}Tc-MAG3) is cleared from the blood by this mechanism, resulting in much higher urinary concentrations and better contrast compared to radiopharmaceuticals eliminated by glomerular filtration [66–69].

3.2.7 Phagocytosis

Phagocytosis is a Greek word for cell eating. It is a process of the cell engulfing a particle and internalizing it. Reticuloendothelial system (RES) cells, such as Kupffer cells in the liver and reticular cells in the spleen, capture and engulf colloidal particles such as Tc-99m sulfur colloid (^{99m}Tc-SC) of particle size range between 0.1–1.0 μm [72, 73]. Focal areas that does not have Kupffer cells, such a tumor, cyst, abscess, or hemangioma, will not have an uptake of ^{99m}Tc-sulfur colloid (cold region) [74].

Also, colloidal particles smaller than 0.1 μm show rapid clearance from the interstitial space

into lymphatic vessels and significant retention in lymph nodes when injected into the interstitial fluid [75]. Cancerous nodes replaced by tumor tissues will not sequester the colloids so no uptake of radioactivity will be visualized (cold region). ^{99m}Tc-antimony sulfide colloid (0.002–0.015 μm), ^{99m}Tc-human serum albumin (0.01–0.02 μm) or ^{99m}Tc-nanocolloid are ideal for lymphoscintigraphic studies [76]. However, these radiotracers are not available in the USA, so passing ^{99m}Tc-SC through 0.2 μm filter is being used for lymphoscintigraphic [76].

3.2.8 Cell Sequestration

Cell sequestration is the process of removal of old or damaged red blood cells from circulation which is mainly associated with the spleen. RBC are labeled with Tc-99m using the commercially available kit, then they are carefully denatured by heating at 49–50 °C for 15 min. Heating RBCs changes their shape from tough biconcave disks to spherocytes with knobby projections and a fragile cell membrane. When they squeeze through the 3 μm pores in the cords of the red pulp they get lysed, releasing their radioactive contents within the spleen. Splenic removal of RBCs is a more selective process than removal by the liver and other RES tissue. This imaging procedure is especially useful for localizing and/or identifying ectopic accessory spleens [77, 78].

3.2.9 Capillary Blockade

Capillary blockade is the physical trapping of particles in capillaries and pre-capillary arterioles (microembolization). The diameter of capillaries and pre-capillary arterioles are about 10 microns and 20–30 microns, respectively, so the radiotracer particles should be a little bigger in size between 15 and 50 microns. The delivery to the capillary is through the blood flow so when the radiolabelled particles are injected intravenously, the lungs are the first capillary encountered. Tc-99m radiolabeled macroaggregated albumin (Tc-99m-MAA) have been used for perfusion lung imaging. The localization in each of the lungs is an indicator for the relative blood flow to each of the two lungs. Therefore, ^{99m}Tc-MAA perfusion lung imaging can also be used to assess blood flow through the pulmonary arteries [79, 80]. If ^{99m}Tc-MAA is injected through a catheter positioned in the hepatic artery, then the hepatic blood flow will deliver it to the capillaries in the liver to evaluate blood flow within the liver [81].

3.2.10 Ion Exchange

Ion exchange is the exchange of ionic chemical analogs. Current radiopharmaceuticals that localize by this mechanism are strontium chloride ($^{89}Sr^{2+}$), a beta-emitter used to treat painful bone metastases, and sodium fluoride ($^{18}F^{-}$), a PET agent used for bone scans [82, 83]. In the hydroxyapaptite of the bone matrix,$^{89}Sr^{+2}$ replaces Ca^{+2} while $^{18}F^{-}$ replaces OH^{-}. Fluoride ions diffuse from the blood compartment and exchange with hydroxyl groups in hydroxyapatite crystal to form fluoroapatite. Uptake of fluoride ion into bone may be due to primary and metastatic tumors as well as bone turnover (metabolism) [82, 83].

3.2.11 Chemisorption

Chemisorption is the binding of phosphate-type compounds onto the surface of the bone. The strength of this binding is intermediate between chemical covalent bonding and hydrogen bonding (adsorption). Radiolabeled diphosponates compounds, ^{99m}Tc-MDP and ^{99m}Tc-HDP are used for bone imaging while ^{153}Sm-EDTMP is used for the treatment of painful bone metastases. Localization is on the surface, therefore, uptake is proportional to the surface area [84, 85]. The larger the surface area of increased bone metabolism, the higher the uptake in that areas such as fracture, infection, and tumor. In addition to chemisorption on the surface of bone, there can also be chemisorption onto calcium phosphate crystals that precipitate in certain soft tissues as a consequence of severe hyperparathyroidism, hypercalcemia, and myocardial infarction.

3.2.12 Cellular Migration

Cellular migration is the directed movement of cells due to stimuli such as the chemotaxis of white blood cells to the site of infection and inflammation. Radiolabeled autologous leukocytes with ^{111}In-oxine or ^{99m}Tc-exametazime (^{99m}Tc-HMPAO) can be used to localize sites of infection similar to the circulating leukocytes due to the attraction of released chemotactic factors [86, 87].

3.2.13 Receptor Binding

Receptor binding is similar to the "lock-and-key" concept. It is the binding of a biological molecule to a specific receptor such as the binding of an antibody or antibody fragment to an antigen and peptides, hormones or neurotransmitter binding to their receptors. Receptor and antigen bindings are very selective and specific; therefore, competition from similar molecules for these receptors and antigens binding is a concern with the possibility saturation. Many tumor cells express antigens or receptors that are expressed in small amounts in normal cells. But tumor cells have higher expression of these antigens and receptors. The localization of radiolabeled antibodies, proteins, hormones, and peptides depend on the blood clearance, tumor blood flow, tumor mass and tumor cell viability. The radionuclide of use should match the pharmacokinetics of the biological molecule. For example, antibodies should be labeled with long half-life radionuclides such as ^{111}In and ^{131}I, while peptides can be labeled with shorter lived radionuclides such as ^{99m}Tc, ^{18}F, or ^{123}I for imaging studies. Iodine-131 is the most used radionuclide for both diagnostic and therapeutic studies. Radioiodide can be labeled on tyrosine residue in the antibody or peptide. However, the other radionuclides are indirectly labeled in which they are coordinated to a chelate such as DTPA or DOTA that is covalently attached to the biological molecule (bifunctional chelating approach).

Antibodies (Ab) are also known as immunoglobulins (Ig) which are a group of glycoprotein molecules produced by B-lymphocytes in response to antigenic stimulation. Ab binds to a specific site of the antigen in which an antigen can have multiple binding sites for different Ab. Although much research has been conducted with radiolabeled antibodies, few are currently marketed. In-111 capromab pendetide (ProstaScint), a monoclonal murine IgG antibody directed to prostate specific membrane antigen (PSMA), is used for staging and follow-up of prostate cancer [88–90]. PSMA is a membrane protein that is expressed in prostate tissue and overexpressed on prostate carcinoma. PSMA has a unique structure consisting of three sections: internal cellular, transmembrane and extracellular portions. ProstaScint was later found to bind to the intracellular epitope of PSMA. Therefore, it was discontinued by the manufacturing company in 2018 after the FDA approved smaller urea-based molecules targeting the extracellular epitope of PSMA. ^{68}Ga-DOTA-PSMA and [^{18}F]PSMA, are the urea-based, low molecular weight inhibitors of PSMA that have replaced ProstaScint [88–90].

^{131}I-tositumomab and ^{111}In/^{90}Y-ibritumomab tiuxetan, are monoclonal murine IgG that bind to CD20 receptors on B-cells and non-Hodgkin's lymphoma tumor cells. These labeled antibodies are used for diagnostic, monitoring, and treatment of non-Hodgkin's lymphoma [91, 92].

Many neuroendocrine tumors have an over expression of somatostatin receptors (SSTR) and there are 5 SSTR subtypes. The two naturally occurring SST peptides, 14 and 28 amino acids long, which are known to have short biological half-life due to enzymatic degradation. A number of biologically stable SST analogues were synthesized. Octreotide analogue is an 8 amino acid long analogue that has a high affinity to 2 and 5 SSTR subtypes. ^{111}In-pentetreotide (Octreoscan), a radiolabeled form of octreotide, is used to detect, localize and evaluate such somatostatin-expressing tumors by binding to these receptors [93]. When octreotide is labeled with ^{90}Y or ^{177}Lu, then it is used for therapeutic purposes. Recently ^{68}Ga-DOTA-octreotide has been approved for PET studies of neuroendocrine tumors [94, 95]. In addition, ^{64}Cu-DOTA-tyr^3-octreotate has been approved as a PET diagnostic agent for neuroen-

docrine tumors but Cu-64 emits β^- so it can be used for therapeutic purposes as well [96].

[^{18}F]Florbetapir (Amyvid, Eli Lilly/Avid Radiopharmaceuticals), [^{18}F]florbetaben (Neuraceq, Piramal Imaging) and [^{18}F]flutemetamol (GE Healthcare. VizamylTM) are radiopharmaceuticals used for patients who are being evaluated for Alzheimer's disease (AD) and other causes of cognitive impairment in the cortical regions and hippocampus. After injection, the tracers diffuse through the blood-brain barrier and binds with high affinity and specificity to β-amyloid neuritic plaques (Aβ aggregates) in the brain of adult patients with cognitive impairment. They rapidly enter the brain and quickly washes out from the brain if not bound to β-amyloid neuritic plaques [97, 98]. These radiotracers share a common imaging target and similar imaging characteristics (Aβ tracers). They can differ in their tracer kinetics, specific binding ratios and optimal imaging parameters therefore, they will have different recommended injected doses, time to initiate imaging post-injection, and scan duration [97, 98].

[^{18}F]Fluoroestradiol ([^{18}F]FES) is an analog of estrogen and is used to detect estrogen receptor-positive breast cancer lesions. It has a high overall sensitivity and specificity in assessing the ER status in breast cancers. [^{18}F]FES uptake has been approved to guide in therapy selection and to predict endocrine treatment response [99].

[^{123}I]ioflupane (DaTscan) is a chemical derivative of cocaine. It binds to presynaptic dopamine transporters, which are primarily located in the striatum. Loss of dopamine transporter density, as occurs in Parkinson's disease, results in reduced uptake of the radiopharmaceutical. The radiotracer localizes to the dopamine transporters in the basal ganglia [100].

3.3 Altered Biodistributions Due to Radiochemical Impurities from Improper Radiopharmaceutical Preparations

Improper preparation can lead to the presence of radiochemical impurities in the final radiopharmaceutical dose. Radiochemical impurities have different pharmacokinetics and biodistributions from the radiopharmaceutical product of interest, and hence these impurities can reduce the image quality while exposing the patients to unnecessary radioactive dose. Therefore it is very important to recognize common radiochemical impurities and their localizations. Table 3.2 lists the main possible radiochemical impurities along with localization site [101].

Table 3.2 Radiopharmaceuticals' predominant radiochemical preparation impurity

Radiopharmaceutical	Predominant radiochemical impurity	Possible localization
^{99m}Tc-radiopharmaceuticals	TcO_4^-	Salivary glands, thyroid, stomach, GI tract, and urine/bladder
	TcO_2 Colloids (particles)	Phagocytized by the liver
^{111}In-radiophamraceuticals	$In(OH)_3$ Colloids (particles)	Phagocytized by liver and spleen
	$^{111}In^{+3}$	Binds to plasma transferrin, and has prolonged blood pool retention
^{123}I/^{131}I-radiopharmaceuticals	$^{123}I/^{131}I^-$	Thyroid
^{18}F-radiopharmaceuticals	$^{18}F^-$	Bone
^{68}Ga-radiophamraceuticals	$^{68}Ga(OH)_3$ Colloids (particles)	Phagocytized by liver and spleen
	$^{68}Ga^{+3}$	Binds to plasma transferrin, and has prolonged blood pool retention

References

1. Kowalsky RJ, Falen SW (2011) Radionuclide production. Radiopharmaceuticals in nuclear pharmacy and nuclear medicine. American Pharmacists Association, pp 31–46
2. Mausner LF, Mirzadeh S (2003) Reactor production of radionuclides. In: Welch M, Redvanly C (eds) Handbook of radiopharmaceuticals radiochemistry and applications. Wiley, pp 87–117
3. Ruth TJ (2003) Accelerators available for isotope production. In: Welch M, Redvanly C (eds) Handbook of radiopharmaceuticals radiochemistry and applications. Wiley, pp 71–85
4. Mahmood A, Jones AG (2003) Technetium radiopharmaceuticals. In: Welch M, Redvanly C (eds) Handbook of radiopharmaceuticals radiochemistry and applications. Wiley, pp 323–325
5. Evans EA (1981) Synthesis of radiolabelled compounds. J Radioanal Chem 64:9–32
6. Bonfils P, Damgaard M, Stokholm KH, Nielsen SL (2012) Tc-99m-albumin can replace I-125-albumin to determine plasma volume repeatedly. Scand J Clin Lab Invest 72:447–451
7. Fairbanks VF, Klee GG, Wiseman GA, Hoyer JD, Tefferi A et al (1996) Measurement of blood volume and red cell mass: re-examination of ^{51}Cr and ^{125}I methods. Blood Cells Mol Dis 22:169–186
8. Berman I, Carr R, Malone E (1964) Determination of total blood volume from measurements of total red blood cell mass and plasma volume, using simultaneously injected isotopes. Nature 202:1013–1015
9. Hambÿe AS, Verbeke KA, Vandermeiren RP, Joosens EJ, Verbruggen AM et al (1997) Comparison of modified technetium-99m albumin and technetium-99m red blood cells for equilibrium ventriculography. J Nucl Med 38:1521–1528
10. Sheakley ML, Gordon L (1984) Evaluation of hepatic hemangioma with Tc-99m labeled red blood cells. J Nucl Med Technol 17:119–121
11. Dong H, Zhang Z, Guo Y, Zhang H, Xu W (2017) The application of technetium-99m-red blood cell scintigraphy in the diagnosis of orbital cavernous hemangioma. Nucl Med Commun 38:744–747
12. Wagner HN, Lopez-Majano V, Langan JK, Joshi RC (1968) Radioactive xenon in the differential diagnosis of pulmonary embolism. Radiology 91:1168–1174
13. Mishkin FS, Brashear RE, Reese IC (1970) Evaluation of regional perfusion and ventilation using xenon 133 and the scintillation camera. Am J Roentgenol 108:60–70
14. Alderson PO, Lee H, Summer WA, Motazedi A, Wagner HN (1979) Comparison of Xe-133 washout and single-breath imaging for the detection of ventilation abnormalities. J Nucl Med 20:917–922
15. Barth A, Haldemann AR, Reubi JC, Rösier H, Kinser JA et al (1996) Noninvasive differentiation of meningiomas from other brain tumours using combined ^{111}indium-octreotide/^{99m}technetium-DTPA brain scintigraphy. Acta Neurochir 138:1179–1185
16. Inoue Y, Momose T, Machida K, Honda N, Mamiya T et al (1993) Delayed imaging of Tc-99m-DTPA-HSA SPECT in subacute cerebral infarction. Radiat Med 11:214–216
17. Balon HR, Fink-Bennett DM, Brill DR, Fig LM, Freitas JE et al (1997) Procedure guideline for hepatobiliary scintigraphy. J Nucl Med 38:1654–1657
18. Rantis PC, Harford FJ, Wagner RH, Henkin RE (1995) Technetium-labelled red blood cell scintigraphy: is it useful in acute lower gastrointestinal bleeding? Int J Colorect Dis 10:210–215
19. Dam HQ, Brandon DC, Grantham VV, Hilson AJ, Howarth DM et al (2014) The SNMMI procedure standard/EANM practice guideline for gastrointestinal bleeding scintigraphy 2.0. J Nucl Med Technol 42:308–317
20. Jian R, Ducrot F, Piedeloup C, Mary JY, Najean Y, Bernier JJ (1985) Measurement of gastric emptying in dyspeptic patients: effect of a new gastrokinetic agent (cisapride). Gut 26:352–358
21. Ertay T, Doğan AS, Ülker Ö, Durak H (2014) In vitro evaluation of Tc-99m radiopharmaceuticals for gastric emptying studies. Mol Imaging Radionucl Ther 23:21–24
22. Nakamura K, Tukatani Y, Kubo A, Hashimoto S, Terayama Y et al (1989) The behavior of ^{99m}Tc-hexamethylpropyleneamineoxime (^{99m}Tc-HMPAO) in blood and brain. Eur J Nucl Med 15:100–107
23. Vanbilloen HP, Cleynhens BJ, Verbruggen AM (1998) Importance of the two ester functions for the brain retention of ^{99m}Tc-labelled ethylene dicysteine diethyl ester (^{99m}Tc-ECD). Nucl Med Biol 25:569–575
24. Berman DS, Kiat H, Maddahi J (1991) The new ^{99m}Tc myocardial perfusion imaging agents: 99mTc-sestamibi and 99mTc-teboroxime. Circulation 84(3 Suppl):I7–I21
25. Braat SH (1991) ^{99m}Tc myocardial perfusion imaging. Curr Opin Radiol 3:810–816
26. Nakamura K, Sammiya T, Hashimoto J, Ishibashi R, Matsumoto K et al (1996) Comparison of cationic myocardial perfusion agents: characteristics of accumulation in cultured smooth muscle cells. Ann Nucl Med 10:375–381
27. Kitsiou NK, Bacharach SL, Bartlett ML, Srinivasan G, Summers RM et al (1999) ^{13}N-ammonia myocardial blood flow and uptake: relation to functional outcome of asynergic regions after revascularization. J Am Coll Cardiol 33:678–686
28. Ziessman H, O'Malley J (2014) Cardiac system. In: Thrall J (ed) Nuclear medicine: the requisites. Elsevier, pp 378–423
29. Hoffer P (1980) Gallium: mechanisms. J Nucl Med 21:282–285
30. Muranaka A, Ito Y, Hashimoto M, Namba M, Nishitani K et al (1980) Uptake and excretion of 67Ga-citrate in malignant tumors and normal cells. Eur J Nucl Med 5:31–37

31. Plathow C, Weber WA (2008) Tumor cell metabolism imaging. J Nucl Med 49(suppl):43S–63S
32. Koopmans KP, Neels ON, Kema IP, Elsinga PH, Links TP et al (2009) Molecular imaging in neuroendocrine tumors: molecular uptake mechanisms and clinical results. Crit Rev Oncol Hematol 71:199–213
33. Neels OC, Koopmans KP, Jager PL, Vercauteren L, van Waarde A et al (2008) Manipulation of [^{11}C]-5-hydroxytryptophan and 6-[^{18}F]fluoro-3,4-dihydroxy-l-phenylalanine accumulation in neuroendocrine tumor cells. Cancer Res 68:7183–7190
34. Masaki Y, Shimizu Y, Yoshioka T, Nishijima K, Zhao S et al (2017) FMISO accumulation in tumor is dependent on glutathione conjugation capacity in addition to hypoxic state. Ann Nucl Med 31:596–604
35. Li F, Joergensen JT, Hansen AE, Kjaer A (2014) Kinetic modeling in PET imaging of hypoxia. Am J Nucl Med Mol Imaging 4:490–506
36. Reske SN, Grillenberger KG, Glatting G, Port M, Hildebrandt M et al (1997) Overexpression of glucose transporter 1 and increased FDG uptake in pancreatic carcinoma. J Nucl Med 38:1344–1348
37. Brown RS, Wahl RL (1993) Overexpression of Glut-1 glucose transporter in human breast cancer: an immunohistochemical study. Cancer 72:2979–2985
38. Rempel A, Mathupala SP, Griffin CA, Hawkins AL, Pedersen PL (1996) Glucose catabolism in cancer cells: amplification of the gene encoding type II hexokinase. Cancer Res 56:2468–2471
39. Caraco C, Aloj L, Chen LY, Chou JY, Eckelman WC (2000) Cellular release of [^{18}F]2-fluoro-2-deoxyglucose as a function of the glucose-6-phosphatase enzyme system. J Biol Chem 275:18489–18494
40. Lan JA, Chervu LR, Johansen KL, Wolkoff AW (1988) Uptake of technetium 99m hepatobiliary imaging agents by cultured rat hepatocytes. Gastroenterology 95:1625–1631
41. Chung JK (2002) Sodium iodide symporter: its role in nuclear medicine. J Nucl Med 43:1188–1200
42. Bizhanova A, Kopp P (2009) Minireview: the sodium-iodide symporter NIS and pendrin in iodide homeostasis of the thyroid. Endocrinology 150:1084–1090
43. Robbins RJ, Schlumberger MJ (2005) The evolving role of 131I for the treatment of differentiated thyroid carcinoma. J Nucl Med 46:28S–37S
44. Drew H, LaFrance N, Chen J (1987) Thyroid imaging studies. J Nucl Med Technol 15:79–87
45. McCall D, Zimmer LJ, Katz AM (1985) Kinetics of thallium exchange in cultured rat myocardial cells. Circ Res 56:370–376
46. Arbab AS, Koizumi K, Toyama K, Arai T, Araki T (1997) Ion transport systems in the uptake of 99Tcm-tetrofosmin, ^{99m}Tc-MIBI and ^{201}Tl in a tumour cell line. Nucl Med Commun 18:235–240
47. Askari A (2019) The sodium pump and digitalis drugs: dogmas and fallacies. Pharmacol Res Perspect 7:e00505
48. Glynn IM, Richards DE (1982) Occlusion of rubidium ions by the sodium-potassium pump: its implications for the mechanism of potassium transport. J Physiol 330:17–43
49. Pandit-Taskar N, Modak S (2017) Norepinephrine transporter as a target for imaging and therapy. J Nucl Med 58:39S–53S
50. Zhang H, Huang R, Cheung NK, Guo H, Zanzonico PB et al (2014) Imaging the norepinephrine transporter in neuroblastoma: a comparison of [^{18}F]-MFBG and 123I-MIBG. Clin Cancer Res 20:2182–2191
51. Weyer K, Nielsen R, Petersen SV, Christensen EI, Rehling M et al (2013) Renal uptake of 99mTc-dimercaptosuccinic acid is dependent on normal proximal tubule receptor-mediated endocytosis. J Nucl Med 54:159–165
52. Willis KW, Martinez DA, Hedley-Whyte ET, Davis MA, Judy PF et al (1977) Renal localization of 99mTc-stannous glucophetonate and 99mTc-stannous dimercaptosuccinate in the rat by frozen section autoradiography: the efficiency and resolution of technetium-99m. Radiat Res 69:475–488
53. Peters AM, Jones DH, Evans K, Gordon I (1988) Two routes for 99mTc-DMSA uptake into the renal cortical tubular cell. Eur J Nucl Med 14:555–561
54. Okudaira H, Shikano N, Nishii R, Miyagi T, Yoshimoto M et al (2011) Putative transport mechanism and intracellular fate of trans-1-amino-3-18F--fluorocyclobutanecarboxylic acid in human prostate cancer. J Nucl Med 52:822–829
55. Ren J, Yuan L, Wen G, Yang J (2016) The value of anti-1-amino-3-18F-fluorocyclobutane-1-carboxylic acid PET/CT in the diagnosis of recurrent prostate carcinoma: a meta-analysis. Acta Radiol 57:487–493
56. Odewole OA, Tade FI, Nieh PT, Savir-Baruch B, Jani AB et al (2016) Recurrent prostate cancer detection with anti-3-[^{18}F]FACBC PET/CT: comparison with CT. Eur J Nucl Med Mol Imaging 43:1773–1783
57. Oka S, Okudaira H, Ono M, Schuster DM, Goodman MM et al (2014) Differences in transport mechanisms of trans-1-amino3-[^{18}F]fluorocyclobutanecarboxylic acid in inflammation, prostate cancer, and glioma cells: comparison with L-[methyl^{11}C] methionine and 2-deoxy-2-[^{18}F]fluoro-D-glucose. Mol Imaging Biol 16:322–329
58. Peck M, Pollack HA, Friesen A, Muzi M, Shoner SC et al (2015) Applications of PET imaging with the proliferation marker [^{18}F]-FLT. Q J Nucl Med Mol Imaging 59:95–104
59. Been LB, Suurmeijer AJ, Cobben DC, Jager PL, Hoekstra HJ et al (2004) [^{18}F]FLT-PET in oncology: current status and opportunities. Eur J Nucl Med Mol Imaging 31:1659–1672
60. Langen KJ, Hamacher K, Weckesser M, Floeth F, Stoffels G et al (2006) O-(2-[^{18}F]fluoroethyl)-L-tyrosine: uptake mechanisms and clinical applications. Nucl Med Biol 33:287–294
61. Pauleit D, Stoffels G, Bachofner A, Floeth FW, Sabel M et al (2009) Comparison of (^{18})F-FET and

(^{18})F-FDG PET in brain tumors. Nucl Med Biol 36:779–787
62. Kennedy EP, Weiss SB (1956) The function of cytidine coenzymes in the biosynthesis of phospholipides. J Biol Chem 222:193–214
63. Kent C (1990) Regulation of phosphatidylcholine biosynthesis. Prog Lipid Res 29:87–105
64. Hara T, Kosaka N, Kishi H (1998) PET imaging of prostate cancer using carbon-11-choline. J Nucl Med 39:990–995
65. DeGrado TR, Baldwin SW, Wang S, Orr MD, Liao RP et al (2001) Synthesis and evaluation of (18) F-labeled choline analogs as oncologic PET tracers. J Nucl Med 42:1805–1814
66. Blaufox MD, Aurell M, Bubeck B, Fommei E, Piepsz A et al (1996) Report of the radionuclides in nephrourology committee on renal clearance. J Nucl Med 37:1883–1890
67. Eshima D, Taylor A (1992) Technetium-99m (^{99m}Tc) mercaptoacetyltriglycine: update on the new ^{99m}Tc renal tubular function agent. Semin Nucl Med 22:61–73
68. Bubeck B, Brandau W, Weber E, Kälble T, Parekh N et al (1990) Pharmacokinetics of technetium-99m-MAG3 in humans. J Nucl Med 31:1285–1293
69. Schaap GH, Alferink TH, de Jong RB, Oe PL, Roos JC et al (1988) ^{99m}Tc-MAG3: dynamic studies in patients with renal disease. Eur J Nucl Med 14:28–31
70. Williams JC (1983) Pertechnetate and the stomach—a continuing controversy. J Nucl Med 24:633–636
71. Chaudhuri TK (1975) Cellular site of secretion of $^{99m}TcO_4$ in the stomach. A controversial point. J Nucl Med 16:1204–1205
72. Higgins CB, Taketa RM, Taylor A, Halpern SE, Ashburn WL (1974) Renal uptake of ^{99m}Tc-sulfur colloid. J Nucl Med 15:564–566
73. Klingensmith WC III, Ryerson TW (1973) Lung uptake of ^{99m}Tc-sulfur colloid. J Nucl Med 14:201–204
74. Prakash R, Gupta RK, Narayanan RV, Chakravarty SK (1989) Technetium-99m radiocolloid scintigraphy, planar and SPECT red blood cell imaging and ultrasonography in diagnosis of hepatic hemangioma. Australas Radiol 33:237–244
75. Oussoren C, Velinova M, Scherphof G, van der Want J, van Rooijen N et al (1998) Lymphatic uptake and biodistribution of liposomes after subcutaneous injection: IV. Fate of liposomes in regional lymph nodes. Biochim Biophys Acta 1370:259–272
76. Hung JC, Wiseman GA, Wahner HW, Mullan BP, Taggart TR et al (1995) Filtered technetium-99m-sulfur colloid evaluated for lymphoscintigraphy. J Nucl Med 36:1895–1901
77. Armas RR (1985) Clinical studies with spleen-specific radiolabeled agents. Semin Nucl Med 15:260–275
78. Atkins HL, Eckelman WC, Hauser W, Klopper JF, Richards P (1972) Splenic sequestration of ^{99m}Tc-labeled red blood cells. J Nucl Med 13:811–814
79. Levine G (1980) Tc-99m MAA: a model for administering the desired number of particles for pulmonary perfusion studies. J Nucl Med Technol 8:33–36
80. Bolstad DM, Valley TB, Wilson ME, Hung JC (1992) An improved technique for reducing the number of particles in a technetium-99m macroaggregated albumin injection. J Nucl Med Technol 20:220–223
81. Ziessman HA, Wahl RL, Juni JE, Gyves JE, Ensminger WD et al (1985) The utility of SPECT for 99mTc-MAA hepatic arterial perfusion scintigraphy. AJR Am J Roentgenol 145:747–751
82. Fukushi Y, Ozawa T, Wakui M, Nishiyama A (1995) Sr^{2+} can pass through Ca^{2+} entry pathway activated by Ca2+ depletion, but can be hardly taken up by the Ca^{2+} stores in the rat salivary acinar cells. Tohoku J Exp Med 176:83–97
83. Czernin J, Satyamurthy N, Schiepers C (2010) Molecular mechanisms of bone 18F-NaF deposition. J Nucl Med 51:1826–1829
84. Subramanian G, McAfee JG, Blair RJ, Kallfelz FA, Thomas FD (1975) Technetium-99m-methylene diphosphonate—a superior agent for skeletal imaging: comparison with other technetium complexes. J Nucl Med 16:744–755
85. Sartor O, Hoskin P, Bruland ØS (2013) Targeted radio-nuclide therapy of skeletal metastases. Cancer Treat Rev 39:18–26
86. Roca M, de Vries EF, Jamar F, Israel O, Signore A (2010) Guidelines for the labelling of leucocytes with (111)In-oxine. Inflammation/infection taskgroup of the European Association of Nuclear Medicine. Eur J Nucl Med Mol Imaging 37:835–841
87. Allan RA, Sladen GE, Bassingham SC, Lazarus SEM, Clarke I et al (1993) Comparison of simultaneous 99mTc-HMPAO and 111In oxine labelled white cell scans in the assessment of inflammatory bowel disease. Eur J Nucl Med 20:195–200
88. Wester HJ, Schottelius M (2019) PSMA-targeted radiopharmaceuticals for imaging and therapy. Semin Nucl Med 49:302–312
89. Lin M, Ta RT, Kairemo K, Le DB, Ravizzini GC (2021) Prostate-Specific Membrane Antigen-Targeted Radiopharmaceuticals in Diagnosis and Therapy of Prostate Cancer: Current Status and Future Perspectives. Cancer Biother Radiopharm 36(3):237–251. https://doi.org/10.1089/cbr.2020.3603. Epub 2020 Jun 23. PMID: 32589458.
90. Okarvi SM (2019) Recent developments of prostate-specific membrane antigen (PSMA)-specific radiopharmaceuticals for precise imaging and therapy of prostate cancer: an overview. Clin Transl Imaging 7:189–208
91. Davies A (2007) Radioimmunotherapy for B-cell lymphoma: Y^{90} ibritumomab tiuxetan and I^{131} tositumomab. Oncogene 26:3614–3628
92. Jacene HA, Filice R, Kasecamp W, Wahl RL (2007) Comparison of ^{90}Y-Ibritumomab Tiuxetan and ^{131}I-Tositumomab in clinical practice. J Nucl Med 48:1767–1776

93. Leners N, Jamar F, Fiasse R, Ferrant A, Pauwels S (1996) Indium- 111-pentetreotide uptake in endocrine tumors and lymphoma. J Nucl Med 37:916–922
94. Deppen SA, Blume J, Bobbey AJ, Shah C, Graham MM, Lee P, Delbeke D, Walker RC (2016) 68Ga-DOTATATE compared with 111In-DTPA-octreotide and conventional imaging for pulmonary and gastroenteropancreatic neuroendocrine tumors: a systematic review and meta-analysis. J Nucl Med 57:872–878
95. Yang J, Kan Y, Ge BH, Yuan L, Li C et al (2014) Diagnostic role of Gallium-68 DOTATOC and Gallium-68 DOTATATE PET in patients with neuroendocrine tumors: a meta-analysis. Acta Radiol 55:389–398
96. Ullrich M, Bergmann R, Peitzsch M, Zenker EF, Cartellieri M et al (2016) Multimodal somatostatin receptor theranostics using [(64)Cu]Cu−/[(177)Lu]Lu-DOTA-(Tyr(3))octreotate and AN-238 in a mouse pheochromocytoma model. Theranostics 6:650–665
97. Yeo JM, Waddell B, Khan Z, Pal S (2015) A systematic review and meta-analysis of (18)F-labeled amyloid imaging in Alzheimer's disease. Alzheimers Dement 1:5–13
98. Auvity S, Tonietto M, Caillé F et al (2020) Repurposing radiotracers for myelin imaging: a study comparing 18F-florbetaben, 18F-florbetapir, 18F-flutemetamol,11C-MeDAS, and 11C-PiB. Eur J Nucl Med Mol Imaging 47:490–501
99. Liao GJ, Clark AS, Schubert EK, Mankoff DA (2016) J Nucl Med 57:1269–1275
100. Roussakis AA, Piccini P, Politis M (2013) Clinical utility of DaTscan™ (123I-Ioflupane Injection) in the diagnosis of Parkinsonian syndromes. Degen Neurol Neuromusc Dis 3:33–39
101. Vallabhajosula S, Killeen RP, Osborne JR (2010) Altered biodistribution of radiopharmaceuticals: role of radiochemical/pharmaceutical purity, physiological, and pharmacologic factors. Semin Nucl Med 40:220–241